

# Laser Sénarmont biascope for residual surface stress measurement of float glasses

T. KISHII

The gas laser-Sénarmont compensator-biascope combination has enabled non-destructive measurement of residual surface stresses in float glasses using the optical waveguide effect in tin-diffused surface layers. The biascope can detect surface stress as low as  $10 \text{ kg cm}^{-2}$ . Annealing and elastic deformation effects in glasses are clearly identified.

KEYWORDS: lasers, biascopes, residual stress, float glass

## Introduction

In their paper<sup>1</sup> and patent description<sup>2</sup>, Acloque and Guillemet gave biascope-Babinet compensator combinations for non-destructive surface stress measurement on tempered glasses.

The author of the present paper has reported that gas lasers improved the biascope sensitivity and applicability<sup>3</sup> and that the biascope could be applied to both flat<sup>3</sup> and curved surfaces<sup>4</sup>. Also, tin-diffused surface layers on plate glasses, produced by the float process, showed a distinct optical waveguide effect<sup>3,5</sup> which could be used for surface stress measurements, both with the biascope<sup>3</sup> and by refractometry<sup>5</sup>.

Surface stress measurements of thermally tempered float glasses by refractometry were reported almost simultaneously by Guillemet<sup>6</sup>, and by the author<sup>7</sup>. The latter insisted that the method could be applied to curved surfaces.

The present paper reports that the gas laser-biascope-Sénarmont compensator combination allows high sensitivity surface stress measurement on float glasses. The combination is effective in detecting or measuring residual surface stress in commercial as-received float glass, surface stress reduction in glass by annealing and stress caused by elastic deformation.

## Experimental methods and principles

### Laser Sénarmont biascope

The optical arrangement of the biascope is shown in Fig. 1. The polarizer, quarter-wave plate and rotatable analyser were combined so that they form a Sénarmont compensator (Fig. 2, and Appendix). The plane of polarization of the polarizer was at  $45^\circ$  with respect to the plane of incidence, and the optical axes  $q$  of the quarter-wave plate were also at  $45^\circ$  with respect to the plane of refraction. The polarizer

could be omitted if the laser emitted linearly polarized light and was so combined that the plane of polarization was at  $45^\circ$  with respect to the plane of incidence.

When the laser beam arrived at the tin-diffused surface from an optically dense input prism, linearly polarized guided mode waves<sup>5</sup> were formed in the surface layer. Some of the waves were refracted back to an optically dense output prism at points on the path. The path of the waves was identified as a bright line in the micrometer field of view, using the refracted light<sup>3</sup>.

### Principle

The important supposition for the present experiment was that the refracted light conserves photoelastic retardations between two linearly polarized component waves of the guided waves at the points of refraction.

When the glass test-piece was stress-free, retardation of both the guided and refracted waves was zero; they were linearly polarized. The refracted light was polarized with planes of polarization at  $45^\circ$  with respect to the plane of refraction (Fig. 2a) and remained linearly polarized after passing through the quarter-wave plate. The bright line in the field of view disappeared completely when the analyser was placed at the crossed-Nicols angle.

When the glass surface was photoelastically birefringent, the incident linearly polarized light became elliptically, circularly or linearly polarized during propagation, depending on the retardation  $R$  between the two linearly polarized component waves (Fig. 2b). The retardation  $R$  was carried by the refracted light which was linearly polarized by the quarter-wave plate. The angles of the polarization planes depended on  $R$ , and could be identified at cut-off caused by analyser rotation; the analyser caused the micrometer image of the light path to disappear near the point where the retardation corresponded to an angle of  $90^\circ$  with the analyser plane.

From the view-point of the observer, the above process could be briefly expressed as follows: the line had a dark

The author is at the Research and Development Centre, Toshiba Corporation, Kawasaki, Japan-210 and also at Toshiba Glass Co, Yoshida, Shizuoka, Japan 421-03. Received 28 January 1982. Revised 28 May 1982

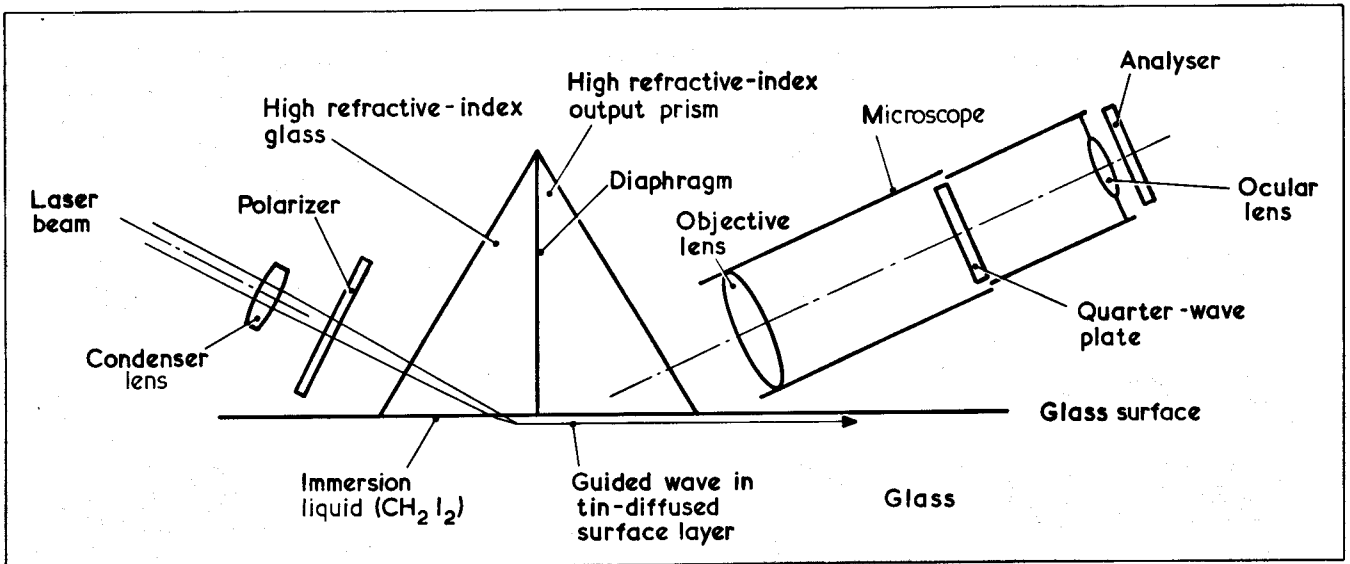


Fig. 1 Laser Sénarmont biascope layout: HeNe laser power is 1 mW; condenser lens  $f = 100$  mm; input high refractive-index glass prism is LAK-10; micrometer objective lens  $f = 40$  mm; ocular micrometer  $\times 10$

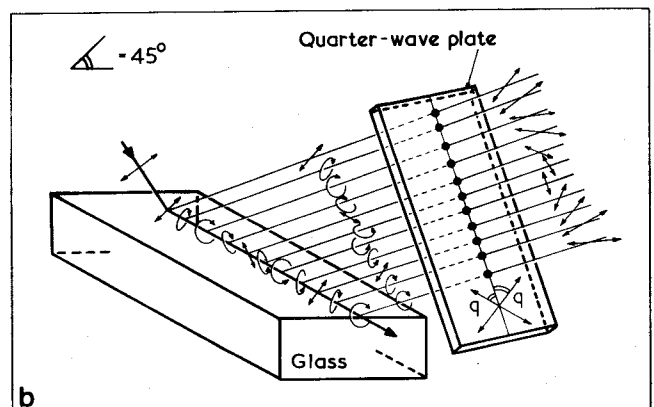
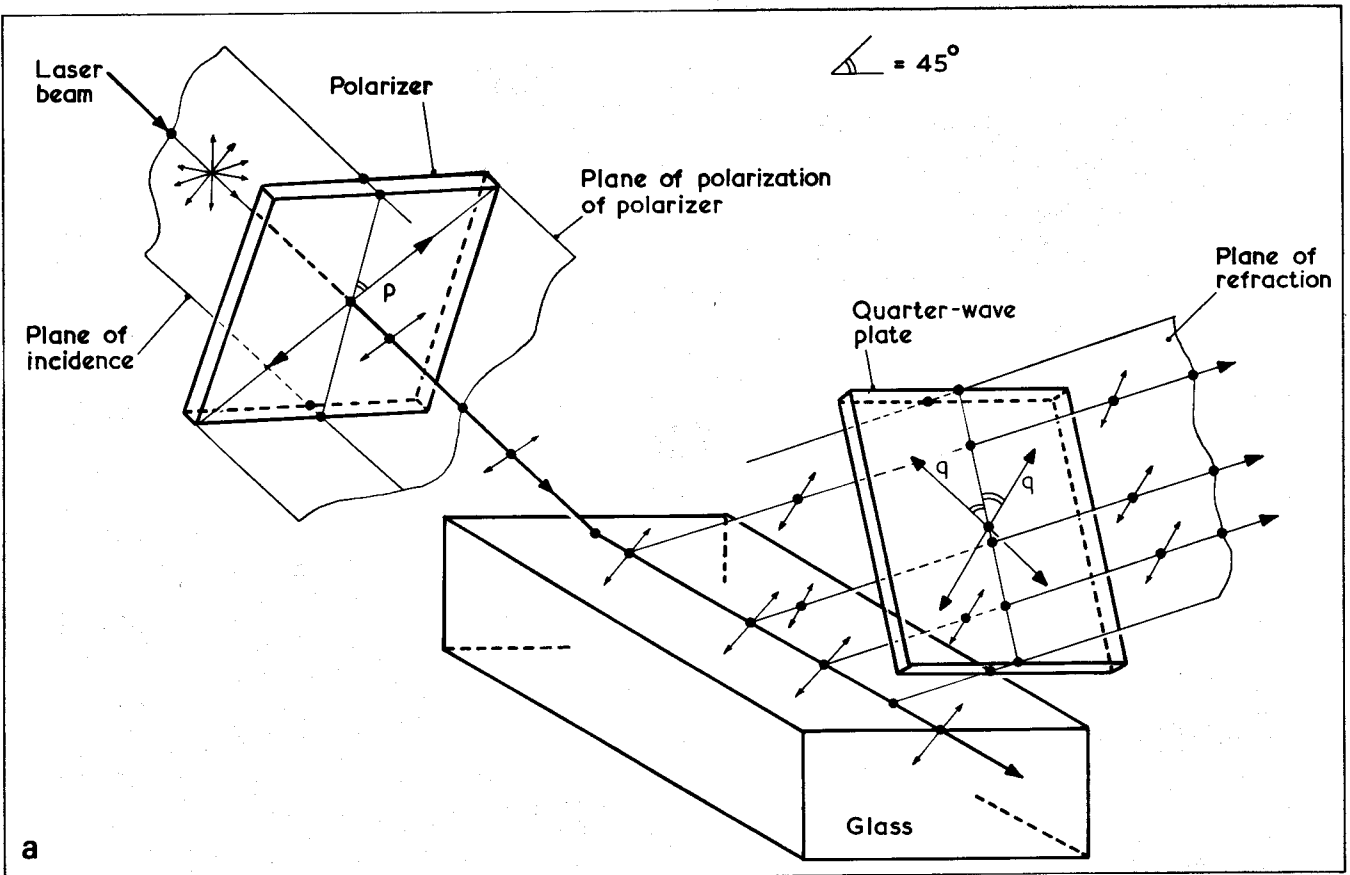


Fig. 2 Schematic diagrams showing optical effects in sample glass and optical system: a — stress-free glass; b — glass with surface stress. p is the polarization axis of the polarizer, q the optical axes of the quarter-wave plate

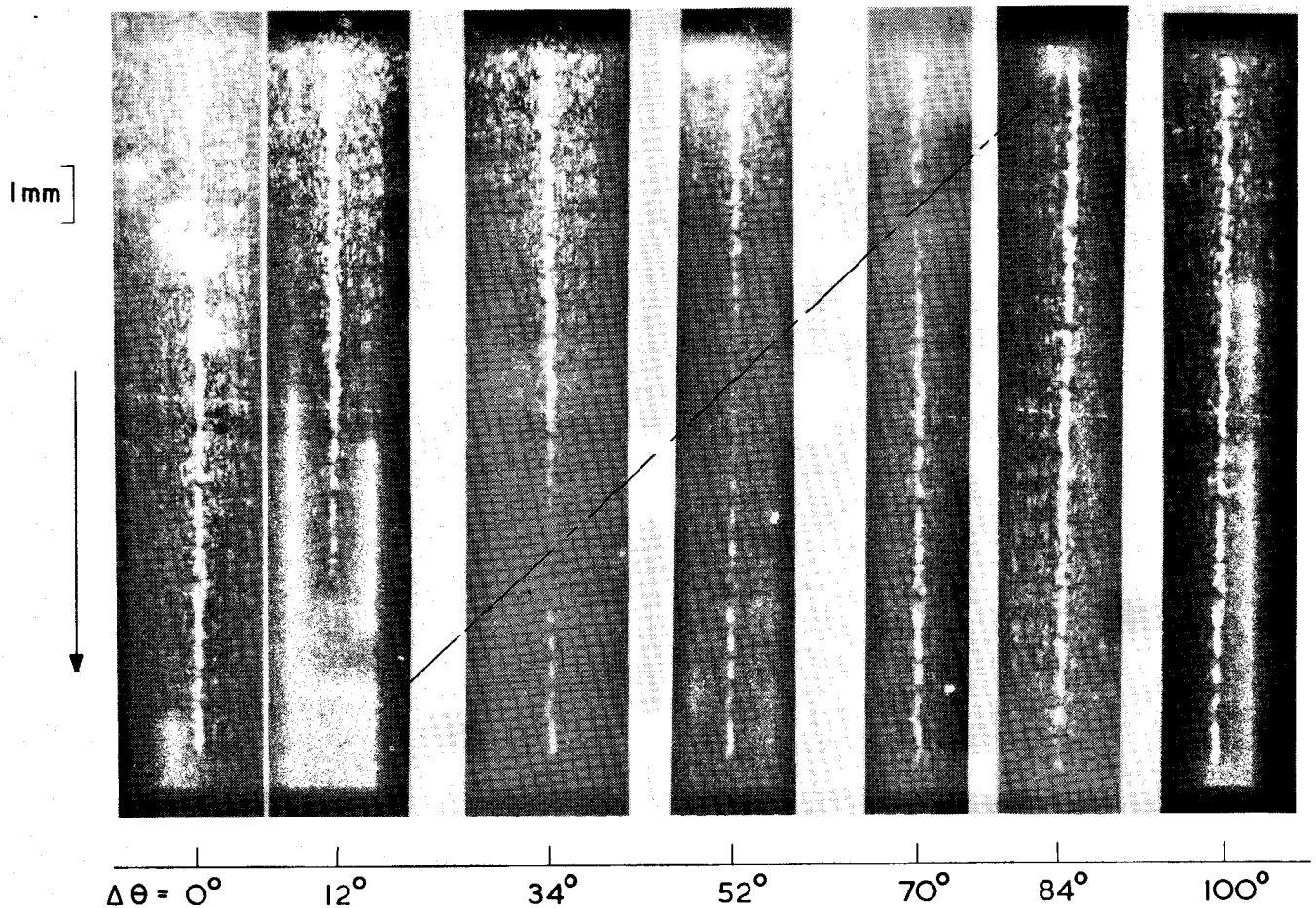


Fig. 3 Sénarmont biascope patterns for an *as-received* float glass 6 mm thick: arrow denotes light propagation direction;  $\Delta\theta$  is the relative analyser angular rotation; — — — — — position of dark portion as a function of analyser rotation  $\Delta\theta$ . Patterns indicate  $69 \text{ kg cm}^{-2}$  surface stress

portion at which photoelastic retardation  $R$  between the two linearly polarized components of the guided waves was compensated for by the Sénarmont compensator.

Analyser rotation of  $\Delta\theta$  shifted the dark portion a distance  $\Delta l$  along the line (Fig. 3).

Surface stress  $F$  is estimated by the following relations:

$$\Delta R = \lambda \frac{\Delta\theta}{180^\circ} \quad (1)$$

$$F = \left( \frac{\Delta R}{\Delta l} \right) / C \quad (2)$$

where  $\Delta R$  is the change in  $R$  (nm) along the path,  $\lambda$  is the wavelength of light (nm) and  $C$  is the photoelastic constant of the glass  $\cong 2.6 \times 10^{-7} (\text{kg cm}^{-2})^{-1}$ . The units of  $\Delta l$  and  $F$  are cm and  $\text{kg cm}^{-2}$  respectively.

As  $\Delta R/\Delta l$  is equal to the photoelastic stress birefringence  $\Delta n$ , (2) can be transformed into

$$F = \Delta n / C \quad (3)$$

The case of  $\Delta\theta = 3^\circ$  and  $\Delta l = 0.5 \text{ cm}$  corresponds to

$$\Delta n = 21 \times 10^{-7} \text{ and } F = 8 \text{ kg cm}^{-2} \quad (4)$$

This stress of  $8 \text{ kg cm}^{-2}$  is far smaller than surface stresses on *as-received* (see results section) and tempered glasses

( $1000\text{--}2500 \text{ kg cm}^{-2}$ ), or tensile strength ( $300\text{--}1000 \text{ kg cm}^{-2}$ ) of glasses, or the sensitivity ( $100 \text{ kg cm}^{-2}$ ) of refractometric surface stress measurement<sup>5</sup>.

#### Cross-section photoelasticity

Cross-sections of float glasses were observed with the conventional linearly polarized method using a Babinet compensator (Figs 4 and 5); namely, a cross-section was examined by passing linearly polarized light through it with the polarization plane at  $45^\circ$  to the float glass surfaces, then through a Babinet compensator and through an analyser so that the usual fringe system was observed.

Surface stresses were estimated by a conventional method<sup>8</sup>; namely, from photoelastic retardations in polarized light passing along the surfaces (for samples with small surface stress) or along central planes (for samples with high surface stress).

#### Annealing

Laboratory-scale annealing operations were carried out using a tubular electric furnace. Glass pieces  $25 \times 25 \text{ mm}$  were heated to  $530^\circ\text{C}$  and then cooled slowly in the furnace.

#### Quenching

Glass pieces  $25 \times 25 \text{ mm}$  were heated to  $600^\circ\text{C}$  or higher and then cooled freely in ambient air, or by mild air blasting, to obtain glasses with various surface stresses.

#### Bending experiment

A float glass strip,  $6 \times 25 \times 120 \text{ mm}$ , was subjected to three-point bending with the tin-diffused surface in tension. Surface

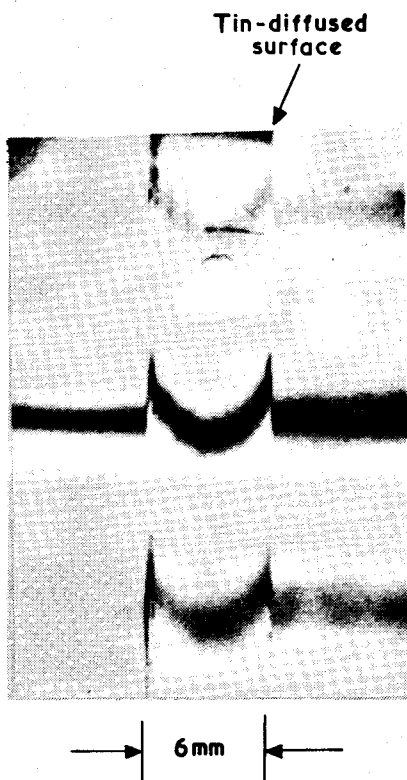


Fig. 4 Cross-section photoelasticity observation for an as-received float glass 6 mm thick. Light paths are 1.45 cm, surface stress was estimated to be  $20 \text{ kg cm}^{-2}$

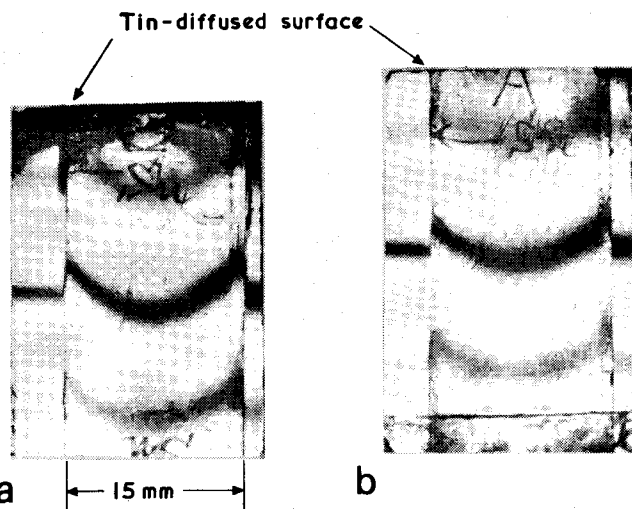


Fig. 5 Cross-section photoelasticity observation for a 15 mm thick float glass: a — before annealing (as-received), surface compression was estimated to be  $22 \text{ kg cm}^{-2}$ . b — after annealing, surface compression estimated to be  $18 \text{ kg cm}^{-2}$ . Light path is 18 mm

stresses were measured at the mid-point in the strip by the biascope.

## Experimental results and discussion

### Effect of residual stress in optical components

The micrometer objective lens (single convex lens), input and output prisms and ocular lens appeared stress-free in a strain viewer based on the linearly polarized light method and the linearly polarized light method with a tinted plate. This corresponded to retardation of less than 3 nm in each optical component.

Surface stress evaluation by  $dR/dI$ , not by  $R$ , excluded the erroneous effect of the input prism.

Table 1. Surface compression values determined by biascope and cross-section photoelasticity

Sample thickness (mm)	Surface compression ( $\text{kg cm}^{-2}$ )	
	Biascope	Cross-section
3	$5_2$	0
6	$6_9$ (Fig. 3)	$2_0$ (Fig. 4)
19	$7_1$	$3_6$

Although the quarter-wave plate was slightly inhomogeneous, it gave no erroneous effect as long as the retardation error was less than  $\lambda/8$  and the cut-off angle of the analyser was used for measurement. This condition was similarly valid for the optical components behind the quarter-wave plate, for example, the ocular lens  $O_m$ .

Significant error was given by the output prism and the objective lens. The maximum retardation, 3 nm, of each component corresponded to  $0.86^\circ$  in  $\Delta\theta$ , or  $1.7^\circ$  for the two components. This was smaller than that used to introduce (4).

### Comparison between biascope and cross-section photoelasticity results

*As-received glasses:* Results are shown in Figs 3 and 4 and in Table 1. In general, the biascope gave higher compression values. Low thermal expansivity for the de-alkalized thin surface layer<sup>5</sup> seemed to be the cause of the higher compression values picked up by the biascope. Although thin sectioning, down to 0.5 mm, failed to identify the surface layer, the result is compatible with results published by Brückner et al<sup>9</sup>.

*Quenched glasses:* For quenched glasses, (Fig. 6) agreement between compression values was satisfactory using both

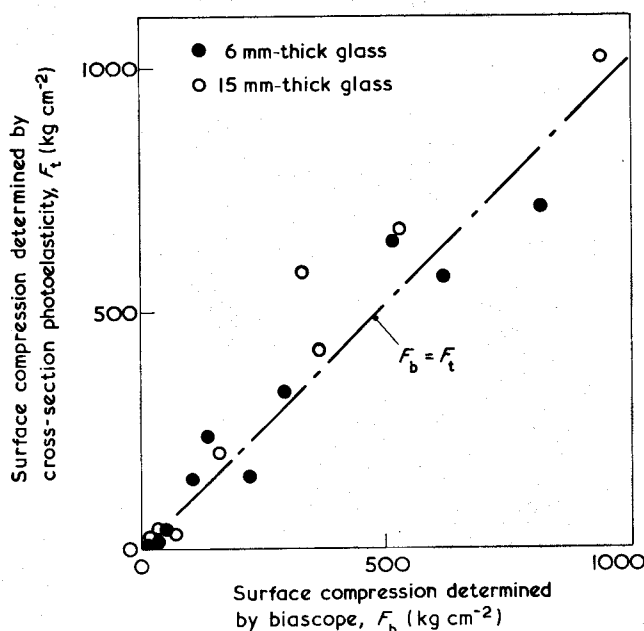


Fig. 6 Comparison between surface stresses on quenched 6 mm thick and 15 mm thick float glasses measured by biascope and by cross-section photoelasticity

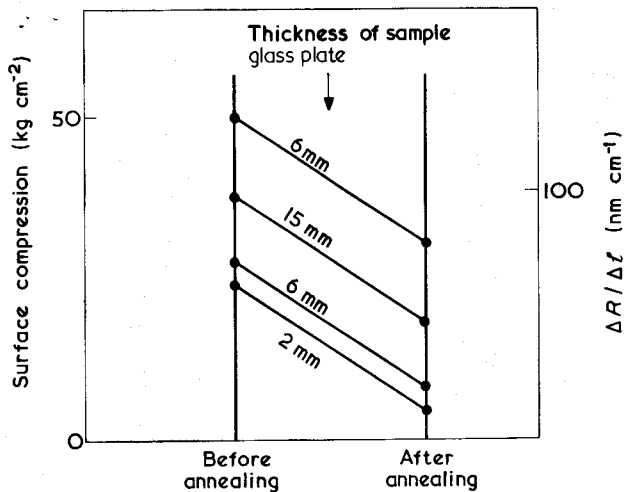


Fig. 7 Surface stresses on float glasses before and after annealing

methods considering local fluctuation in surface stress distribution for the glasses.

**Annealing effect:** Surface stress reduction by annealing was evident both with the biascope (Fig. 7) and by cross-section photoelasticity (Fig. 5), although stress values determined by both methods were not coincident with each other, as described for as-received and quenched glasses.

**Elastic deformation effect**

Stress values obtained with the biascope and by calculation are compared in Fig. 8. The figure indicates that residual surface compression for an as-received glass was cancelled but the tension returned upon loading. The surface stress was the algebraic sum of residual compression and elastic tension.

**Conclusion**

Experimental results in the preceding section have shown that the laser Sénarmont biascope was sensitive enough to

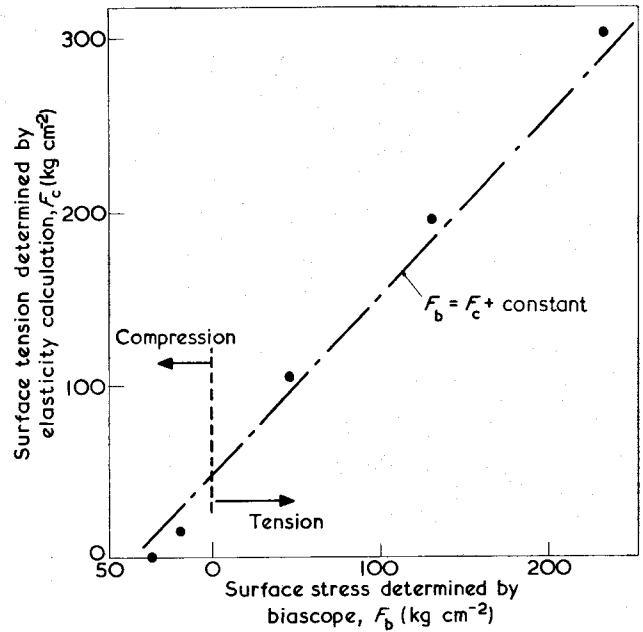


Fig. 8 Surface stress change by elastic deformation

measure residual surface stress, and to detect stress reduction by annealing, in float glasses. Surface layers with higher compressions were detected in the glasses. The biascope seemed useful in both factory and laboratory experiments. Potential application areas appear to be laminated automobile windshield glass or evacuated electronic tubes.

**Appendix**

Figure 9 shows the Sénarmont method used in an ordinary photoelastic measurement by transmitted light. Monochromatic light of wavelength  $\lambda$  propagates through a polarizer, glass test-piece, quarter-wave plate and a rotatable analyser.

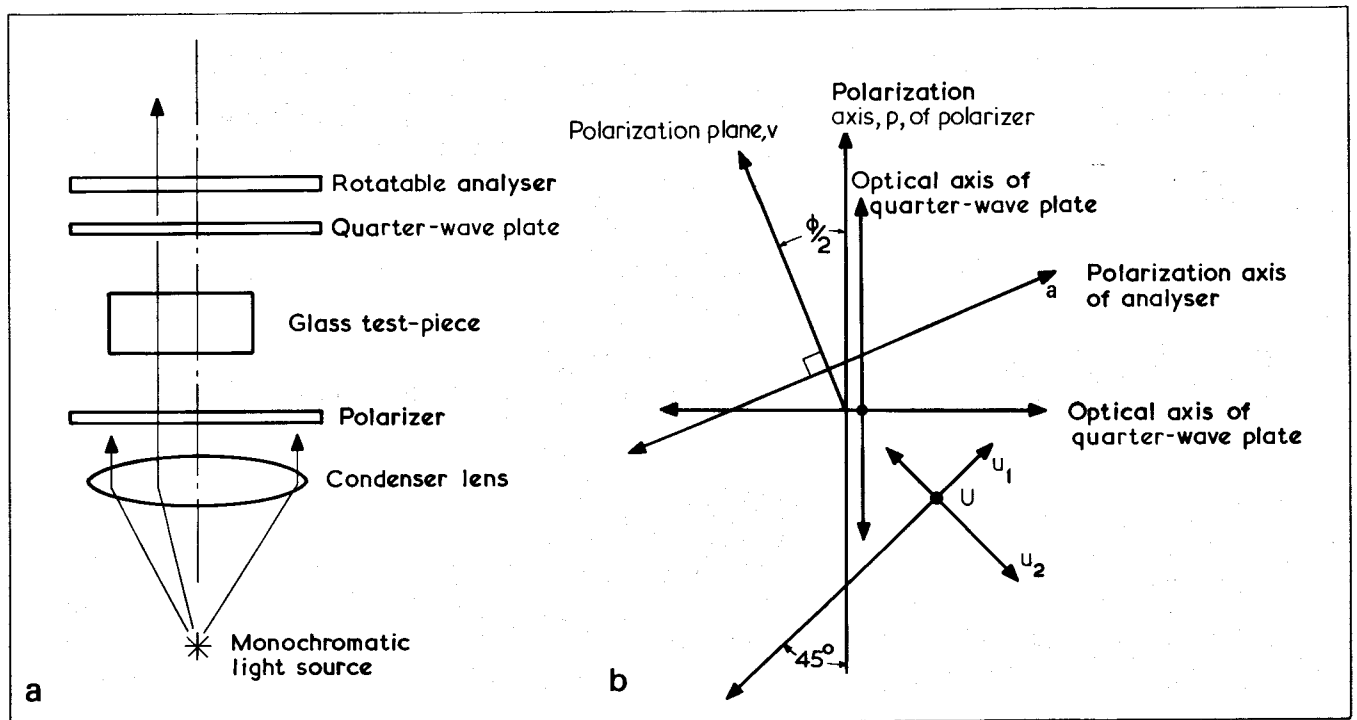


Fig. 9 Optical components in Sénarmont method: a — vertical view; b — horizontal view. U is a point in the glass test-piece and  $u_1, u_2$  are principal stress axes at U, v is the polarization plane of the linearly polarized light which propagates from Q to A, and a is the polarization of the analyser which brings the point U to cut-off

axis  $p$  of the polarizer, and the principal stress axes  $u_1$  and  $u_2$  at the point  $U$  to be tested in the test-piece are at  $45^\circ$  to  $p$ .

Linearly polarized light from the polarizer passes through the glass test-piece via  $U$  where the stress field produces a retardation  $R$  (or angular retardation  $\phi$ ) between two linearly-polarized component waves of the incident linearly polarized light such that the light becomes linearly polarized ( $\phi = 0^\circ, 90^\circ, 180^\circ$ , etc), circularly polarized ( $\phi = 45^\circ, 135^\circ$ , etc) or elliptically polarized. It is again linearly polarized after passing through the quarter-wave plate, the polarization plane  $v$  of which is at an angle  $\phi/2$  to the axis  $p$ .

The angle  $\phi/2$  is identified at cut-off caused by analyser rotation: when the point  $U$  is within a dark fringe the polarization axis of the analyser is at  $90^\circ$  to the polarization plane  $v$  which is at  $\phi/2$  to  $p$ .

The angular retardation  $\phi$  (in degrees) is converted to linear

retardation  $R$  by  $\lambda\phi/360^\circ$ , or in other words

$$R = \lambda \frac{\phi/2}{180^\circ}$$

## References

- 1 Acloque, P., Guillemet, C. *Silikattechnik* 11 (11) (1960) 502
- 2 Acloque, P., Guillemet, C. US Patent No 3 286 581 (1966)
- 3 Kishii, T. *Opt Laser Technol* 13 (1981) 261
- 4 Kishii, T. *Yogyo-Kyokai-Shi (J Ceram Soc Japan)* 89 (1981) 363
- 5 Kishii, T. *Opt Laser Technol* 11 (1979) 259
- 6 Guillemet, C. Proc symp on optical methods in mechanics of solids, Sijthoff & Noordhoff, Netherlands (1981) 645
- 7 Kishii, T. Presented at the Osaka regional meeting of the Ceram Soc Japan (20th Oct, 1978). Published in Ref. 5 (Oct, 1979)
- 8 Gardon, R. 'Comptes Rendus VII<sup>e</sup> Congress Intern. due Verre' chap. 79 (1965)
- 9 Brückner, R., Navarro, J.F. *Glastech Ber* 44 (1971) 361